

Stellar Physics (radiative processes): dust and radiation

辜品高

gu@asiaa.sinica.edu.tw

Interaction of a grain with radiation

Electric properties of solids are introduced by ε (dielectric constant),
 μ (magnetic permeability), and hence the refractive index $n = \sqrt{\varepsilon\mu}$ in the Maxwell eqns.

grain with the refractive index $n(\nu) = n_R(\nu) + in_I(\nu)$

in vacuum: $E = E_0 \exp[i(kx - \omega t)]$ with $c = \frac{\omega}{k}$

in the grain: $E = E_0 \exp[i((n_R\omega/c)x - \omega t)] \exp[-(n_I\omega/c)x]$ with $\frac{c}{n} = \frac{\omega}{k}$

$n = \sqrt{\varepsilon\mu} \approx \sqrt{\varepsilon}$, where $\varepsilon (= \varepsilon_R + i\varepsilon_I)$.

$\Rightarrow \varepsilon_R = n_R^2 - n_I^2, \quad \varepsilon_I = 2n_R n_I$

N.B. $\varepsilon = 1 + 4\pi\chi_e, \quad \vec{P} = \chi_e \vec{E}$

Cross section of grains

consider spherical grains

$$\sigma_{\nu,ext} = \sigma_{\nu,abs} + \sigma_{\nu,sca} = \pi a^2 Q_{abs} + \pi a^2 Q_{sca},$$

where Q_{abs} and Q_{sca} are the absorption and scattering efficiencies, respectively.

As expected from the previous slide, Q depends on material properties and through $n(\nu)$, which have been measured in the lab. Although there is no simple formula, there are general properties about Q (Mie theory):

$$x \equiv 2\pi a / \lambda$$

For $x \gg 1$, $Q_{abs} \sim Q_{sca} \sim 1 \Rightarrow Q_{abs} + Q_{sca} \sim 2$ (Babinet's Principle)

For $x \ll 1$, $Q_{abs}(a, \nu) \sim 4x \operatorname{Im} \left(\frac{n^2 - 1}{n^2 + 2} \right) \propto \nu^\beta$ ($\beta \approx 1-2$),

$$Q_{sca}(a, \nu) \sim \frac{8}{3} x^4 \operatorname{Re} \left[\left(\frac{n^2 - 1}{n^2 + 2} \right)^2 \right] \quad (\text{Rayleigh scattering})$$

Evans: The Dusty Universe

cf. Figure 3.9 in Rybicki & Lightman

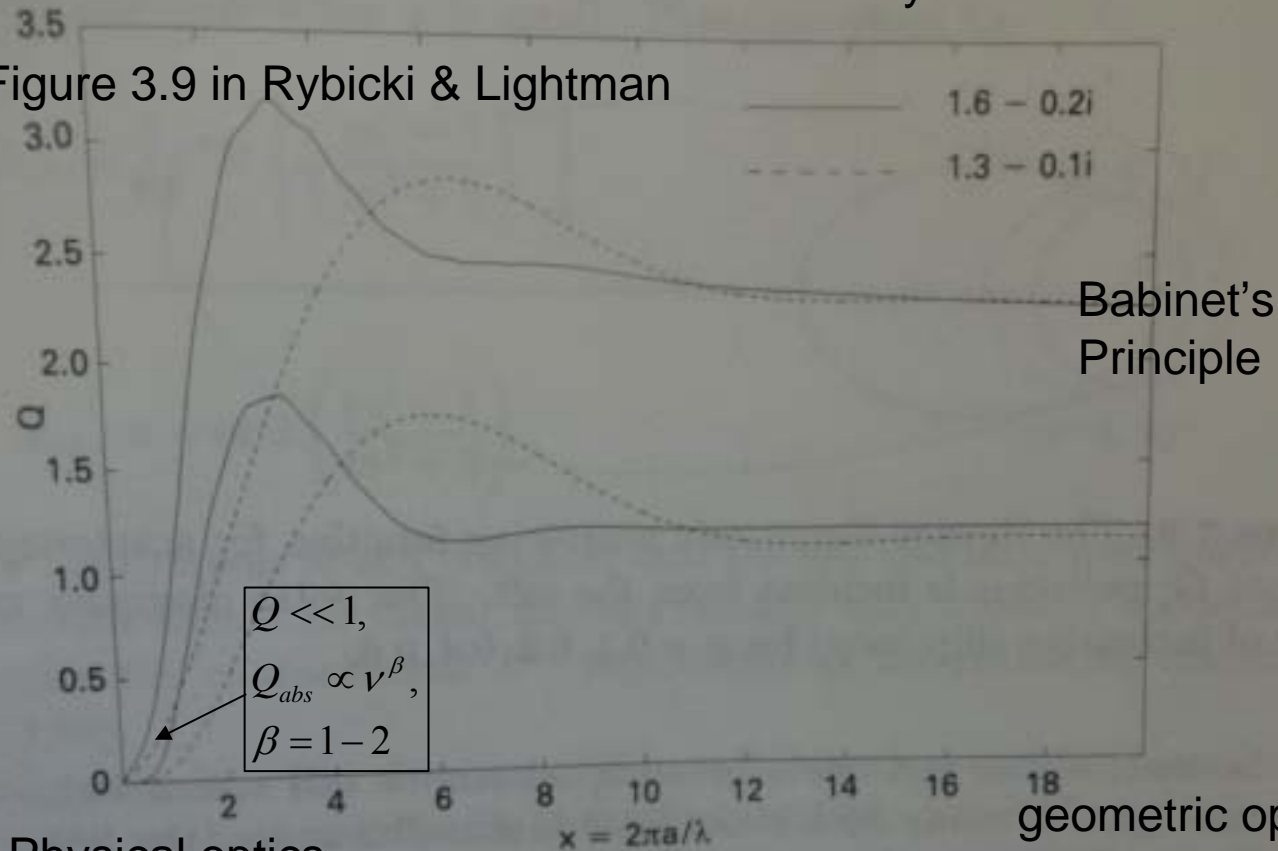


Figure 3.7: Dependence of optical efficiencies Q_{ext} and Q_{sca} on $x = 2\pi a/\lambda$. Refractive indices as indicated; Q_{ext} is the upper curve in each case.

Babinet's Principle

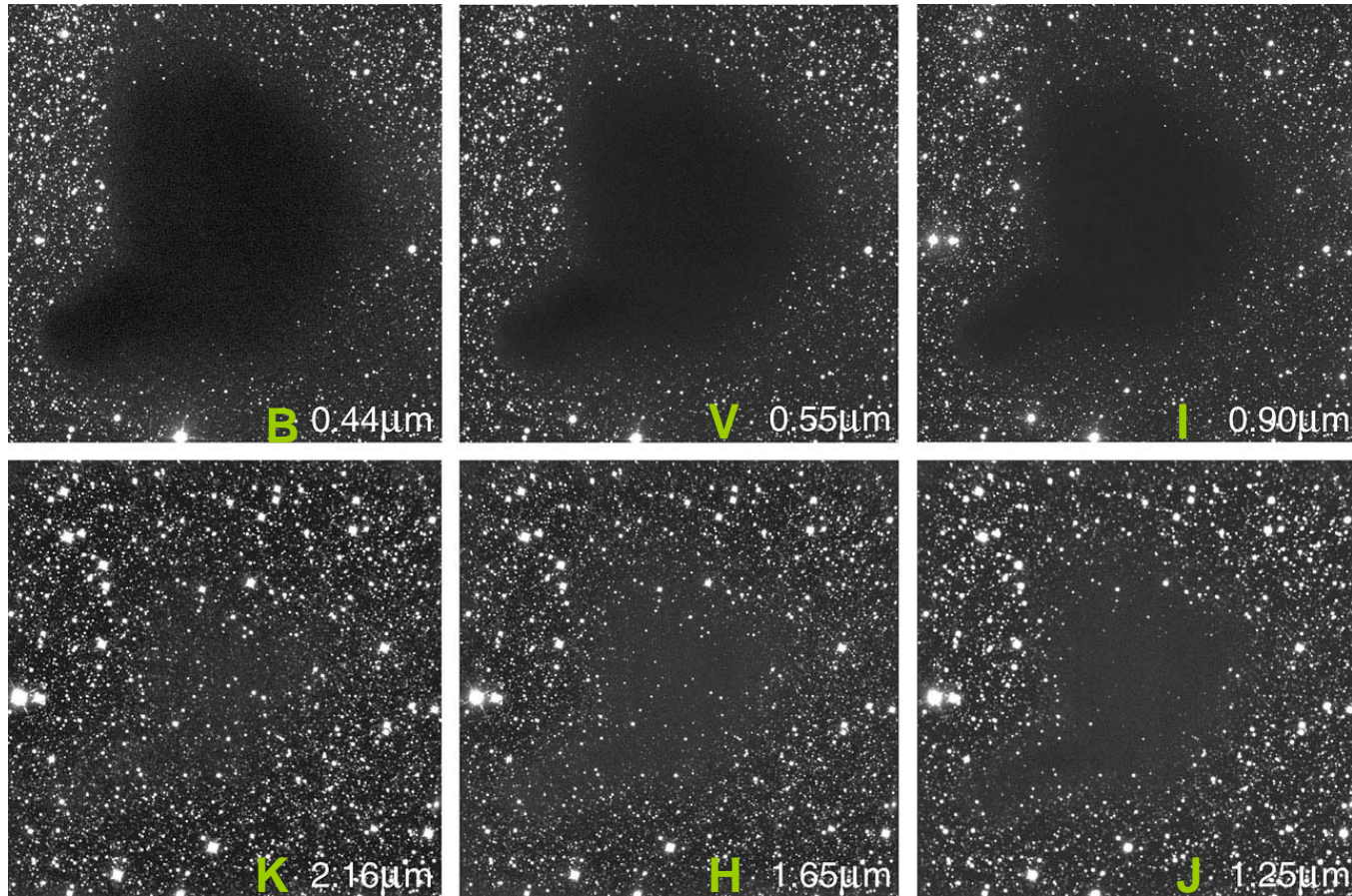
$$\text{When } a \gg \lambda, \quad Q_{abs} + Q_{sca} = 2.$$

The proof of this goes as follows: suppose we have an infinite plane wave focused by an infinite lens onto a point on a wall. The power pattern should be a delta function at that point on the wall. Now suppose you place a screen with an aperture of diameter a between the plane wave and the lens. We should now see an interference pattern on the wall. Call the power incident on a point on the wall $P1$. Now put in a new aperture which is the exact complement of our previous one (it is a scattering body of diameter a), we should see a new power at our point on the wall: $P2$. However, the sum of waves incident on the wall under these two apertures should be the same as the wave from the sum of the apertures, which was a delta function. Thus: $P1=P2$. The first aperture (the slit) represented the scattering power from diffraction alone ($Q_{sca} = 1$), and the second represented the absorbed power. The sum of these two powers, for everywhere but the true focus point, is actually twice the incident power, and since $P1 = P2$, we get: $Q_{sca} + Q_{abs} = 2$. Note that if $Q_{sca} > 1$, then the object is "shiny": more light gets diffracted and less gets absorbed. Thus, although Q_{sca} changes, the sum remains the same.

Interstellar dust size

<http://www.eso.org/public/images/eso9934b/>

Black Cloud B68



The size of most of interstellar dust should be $< 1 \mu\text{m}$

Gas in dark clouds

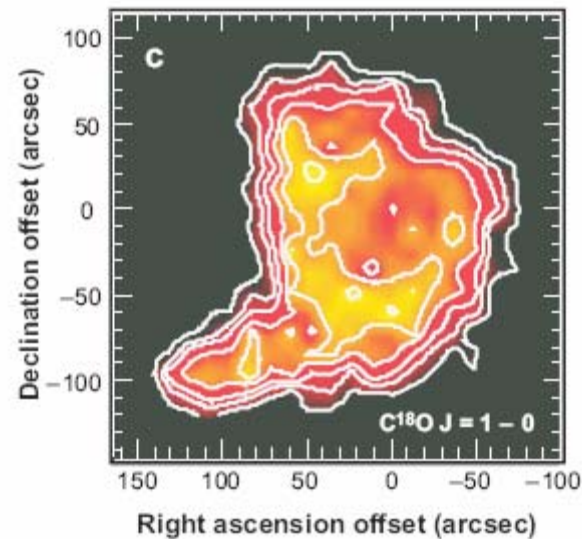
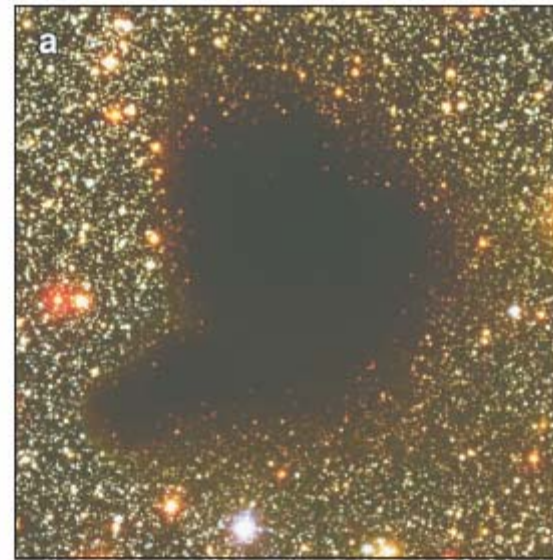
Bergin et al. (2002)

Dust grains ($\sim 0.1 \mu\text{m}$ size, silicates or carbonaceous material $\approx 1\%$ by mass of ISM)

Dust required for H_2 formation

Dusty region (region of extinction) are coincident with molecular clouds as defined by CO

Molecular clouds: the coldest objects in the universe



Dust extinction (UV, Optical, NIR)

extinction = absorption + scattering

extinction only $\Rightarrow I_\nu(\tau) = I_\nu(0) \exp(-\tau_\nu)$

magnitude: $m_\nu = -2.5 \log I_\nu + \text{const.}$

Extinction: $A_\nu = m_\nu(\tau) - m_\nu(0)$

$$= -2.5[(\log I_\nu(0) \exp(-\tau_\nu)) - \log I_\nu(0)]$$

$$= (2.5 \log e) \tau_\nu = 1.086 \tau_\nu$$

distance modulus: $m_\nu - M_\nu = 5 \log D(\text{pc}) + A_\nu - 5$

note that D has large uncertainties to obtain A_ν ,

especially for longer wavelengths. Strategy: use colors!

color excess/reddening: $E(\lambda - V) \equiv A_\lambda - A_V = (m_\lambda - m_V) - (M_\lambda - M_V)$

\Rightarrow obtain $E(\lambda - V)$ as a function of λ ,

which can be seen in the previous slide for B68.

N.B. at NIR, dust thermal emission around a star

could exist due to a protoplanetary or debris disk

besides interstellar extinction.

known from
spectral type
of a star

observed

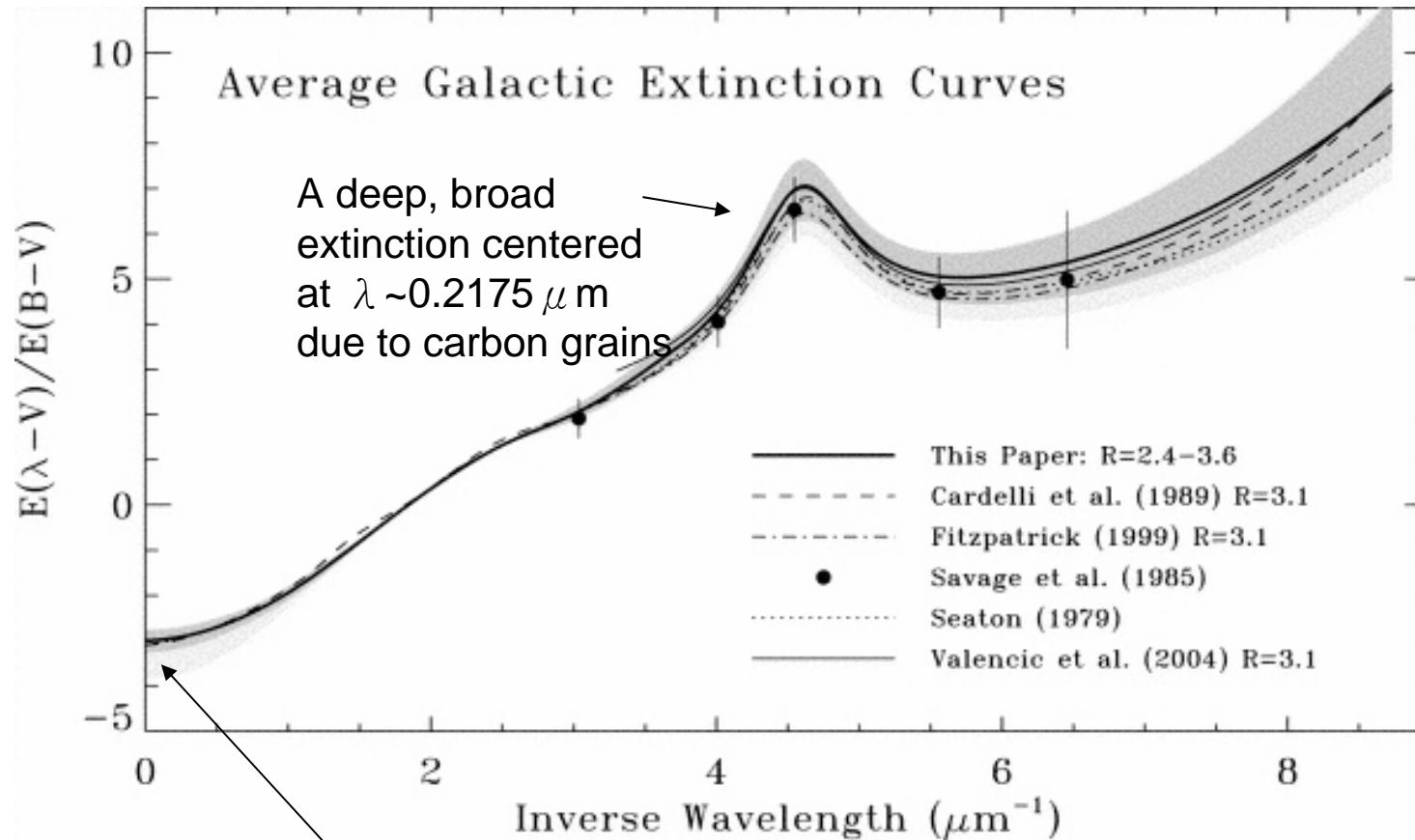
normalized extinction

$$\frac{E(\lambda - V)}{E(B - V)} = \frac{A_\lambda - A_V}{A_B - A_V} = \frac{\tau_\lambda - \tau_V}{\tau_B - \tau_V} = \frac{\sigma_\lambda - \sigma_V}{\sigma_B - \sigma_V}$$

i.e. the normalization factor $E(B - V)$ filters out the dust column density ($N_d = \int n_d dl$) of the ISM between a star and the observer. Thus, one can observe many stars at different distances to construct the normalized extinction curve as a function of λ .

Extinction curve in MW

Fitzpatrick & Massa (2007): reddening increases with shorter wavelength



$$Q_{ext} \rightarrow 0 \text{ as } \lambda \rightarrow \infty: \frac{E(\infty - V)}{E(B - V)} = \frac{-A_V}{E(B - V)} \equiv -R_V \Rightarrow R_V \approx 3.1 \text{ (diffuse interstellar grains)}$$

Measure extinction

$$\frac{A_V}{E(B-V)} = R_V$$

$$\Rightarrow A_\lambda = E(\lambda - V) + A_V = E(\lambda - V) + E(B - V)R_V$$

Extinction curves in nearby galaxies

Pei (1992)

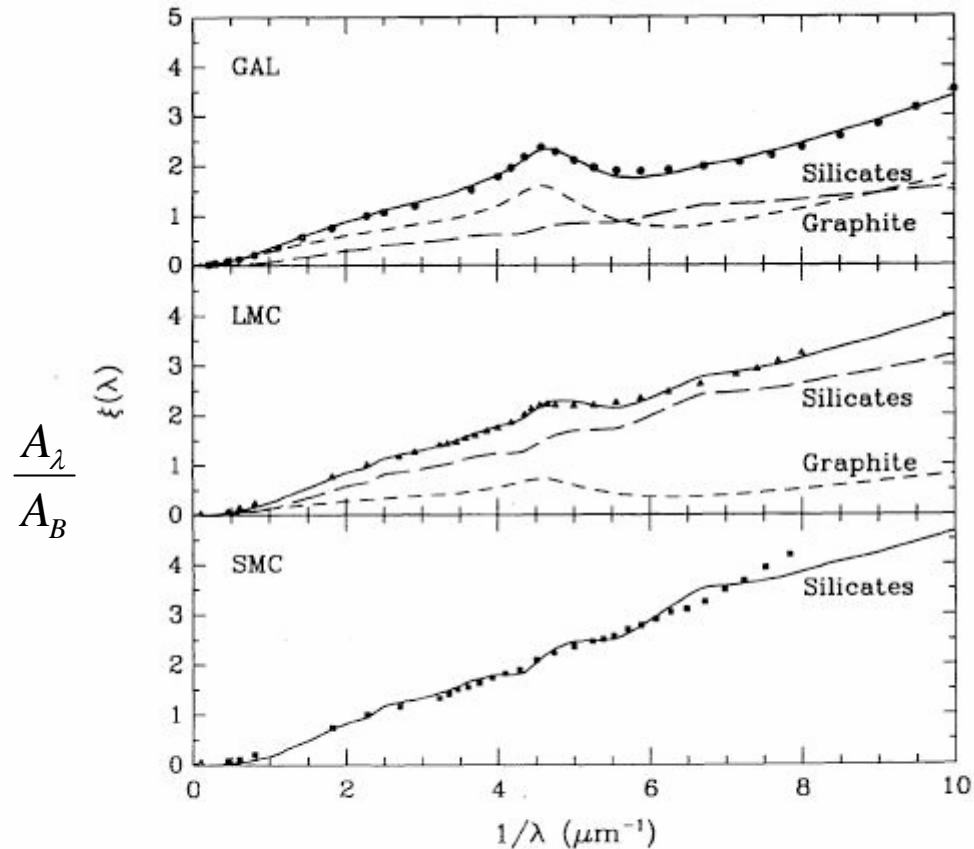


FIG. 5.—Comparisons between the model and empirical extinction curves in the Milky Way, LMC, and SMC. The short and long-dashed lines show, respectively, the relative contributions from graphite and silicate grains, with the sum of the two shown as the solid lines.

Fitting :

ISM grain size distribution

$$n(a) \propto a^{-3.5}$$

$$a_{\min} = 0.005 \mu\text{m}$$

$$a_{\max} = 0.25 \mu\text{m}$$

(Mathis et al. 1977)

Extinction curves are not just give extinction/color excess, but can also constrain dust properties (e.g. size distribution, composition)!

dust temperature

dust can be heated by radiation, impact of atoms/ions, chemical reactions on grain surfaces. In the following, we focus only on radiative heating.

suppose that a grain is like a black body $\Rightarrow (\sigma T_*^4 4\pi R_*^2)(\pi a^2 / 4\pi r^2) = 4\pi a^2 \sigma T_d^4 \Rightarrow (R_* / 2r)^{1/2} T_*$,
 r is the distance between the dust grain and the star.

However, dust grains do not absorb and radiate like blackbodies; they are too small! Generally speaking, they act like a blackbody only at shorter wavelengths, i.e. absorption will be most efficient when $\lambda \ll a$ (optical - UV). Mathematically, the efficiency with which a grain absorbs and emits radiation is determined by Q_{abs} .

Assume a dust grain in thermal equilibrium : heating rate = cooling rate, & Kirchoff's law $j_\nu = \alpha_\nu B_\nu(T_\nu)$,

$$\text{namely, } \dot{E}_{abs} = \dot{E}_{emit} \Rightarrow \int_0^\infty \frac{L_*(\nu)}{4\pi r^2} \pi a^2 Q_{abs}(a, \nu) d\nu = \int_0^\infty 4\pi [\pi a^2 Q_{abs}(a, \nu)] B_\nu(T_d) d\nu$$

Note that the integrand in \dot{E}_{emit} can be rearranged to $(4\pi a^2) Q_{abs}(\pi B_\nu)$, indicating that Q_{abs} also bears the meaning of the emissivity of a dust grain.

Generally, $Q_{abs}(a, \nu)$ depends on temperature and the determination of T_d has to be carried out numerically. Nevertheless, some simplification can be done.

dust temperature

Let's define the Planck mean of Q_{abs} :

$$\bar{Q}_{abs}(a, T) = \frac{\int_0^\infty Q_{abs}(\nu, a) B_\nu(T) d\nu}{\int_0^\infty B_\nu(T) d\nu} = \frac{\int_0^\infty Q_{abs}(\nu, a) B_\nu(T) d\nu}{\sigma T^4 / \pi}$$

Then the energy balance equation for a dust grain becomes

$$\frac{4\pi R_*^2}{4\pi r^2} \pi a^2 \bar{Q}_{abs}(T_*, a) \frac{\sigma T_*^4}{\pi} = 4\pi^2 a^2 \bar{Q}_{abs}(T_d, a) \frac{\sigma T_d^4}{\pi} \Rightarrow T_d = \left(\frac{L_*}{16\pi r^2 \sigma} \frac{\bar{Q}_{abs}(T_*, a)}{\bar{Q}_{abs}(T_d, a)} \right)^{1/4}.$$

Assume $Q_{abs}(\nu, a) \propto a \nu^\beta \Rightarrow \bar{Q}_{abs} \propto a T^\beta$.

In general, $\bar{Q}_{abs} = \min[1, AaT^\beta]$ with A is a constant (e.g. see the figure on next slide).

Use $\bar{Q}_{abs}(T_*, a) = 1$ ($x \gg 1$) and $\bar{Q}_{abs}(T_d, a) = AaT_d^\beta$ ($x \ll 1$) $\Rightarrow T_d = \left(\frac{L_*}{16\pi r^2 \sigma} \frac{1}{Aa} \right)^{1/(\beta+4)}$. note that $T_{d,small} > T_{d,large}$.

However for very small grains such that $AaT^\beta < 1$ even at T_* $\Rightarrow T_d = \left(\frac{L_* T_*^\beta}{16\pi r^2 \sigma} \right)^{1/(\beta+4)} = \left(\frac{R_*}{2r} \right)^{2/(4+\beta)} T_*$

If $\beta = 0$ (black body), $T_d \propto r^{-1/2}$. Thus T_d falls off more slowly with r than does the black body temperature. Dust grains are thus much warmer than they would be if they were black bodies : they can absorb starlight (mostly at optical) quite efficiently, but since they are cool themselves, their emission is mostly at long wavelengths, where they are very inefficient emitters.

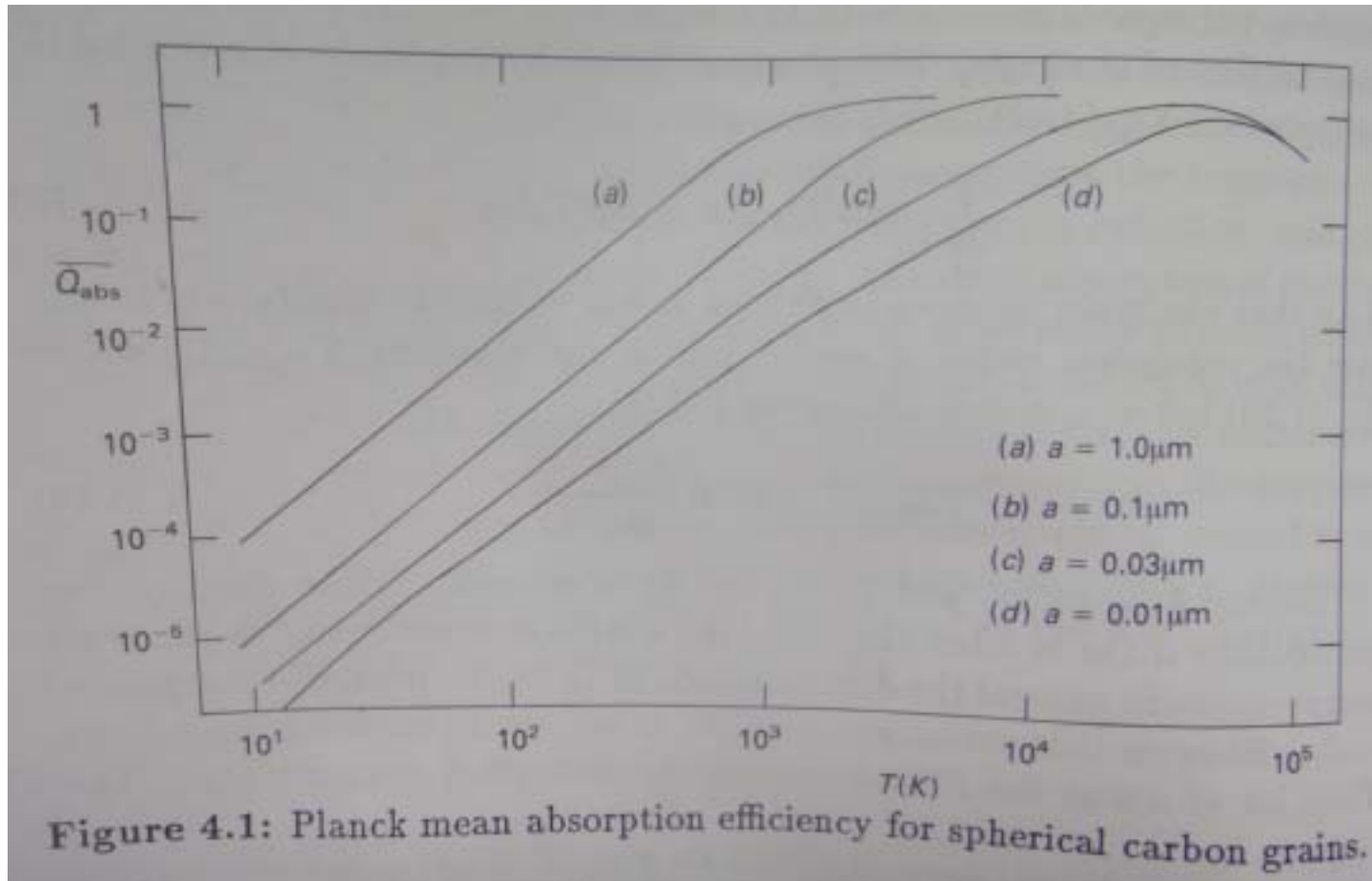


Figure 4.1: Planck mean absorption efficiency for spherical carbon grains.

A. Evans: The Dusty Universe

Dust temperature

The previous estimate of the dust temperature is more relevant to circumstellar dust. However, an interstellar grain is clearly not heated by a single star, but is heated by radiation from general background starlight; i.e. radiation comes from a few point sources (stars) scattered more-or-less at random over the space. Therefore the source of radiative heating in the energy balance equation for dust should be replaced by the interstellar radiation field (ISRF).

Let F_ν the incident interstellar flux on a spherical grain

$$\dot{E}_{abs} = \int 4\pi a^2 Q_{abs} F_\nu d\nu, \text{ where } F_\nu = \pi I_\nu = \pi J_\nu = \frac{c u_\nu}{4\pi}$$

$$u_{ISRF} = \int u_\nu d\nu \sim 10^{-12} \text{ erg/s}$$

A more detailed calculation of the dust temperature as a function of dust size and composition (graphite or silicate) can be found in Draine & Lee (1984). Typical T_d is 12-20 K for $a = 1$ to $0.01 \mu\text{m}$. Note that in the massive star forming regions, T_d can be over 100 K due to high ISRF.

Dust thermal emission

dust emission is given by the solution to the radiative transfer eqn :

$$I_\nu = I_\nu(0) \exp(-\tau_\nu) + S_\nu [1 - \exp(-\tau_\nu)] = 0 + B_\nu(T_d) [1 - \exp(-\tau_\nu)],$$

where $\tau_\nu = \int \pi a^2 Q_{ext}(a, \nu) n(a) da dl$.

At long λ (e.g. FIR, sub - mm), the emission is dominated by large, cold dust grains. Because the dust is very optically thin at these λ :

$$I_\nu = B_\nu(T_d) \tau_\nu, \text{ which is equivalent to considering emission only;}$$

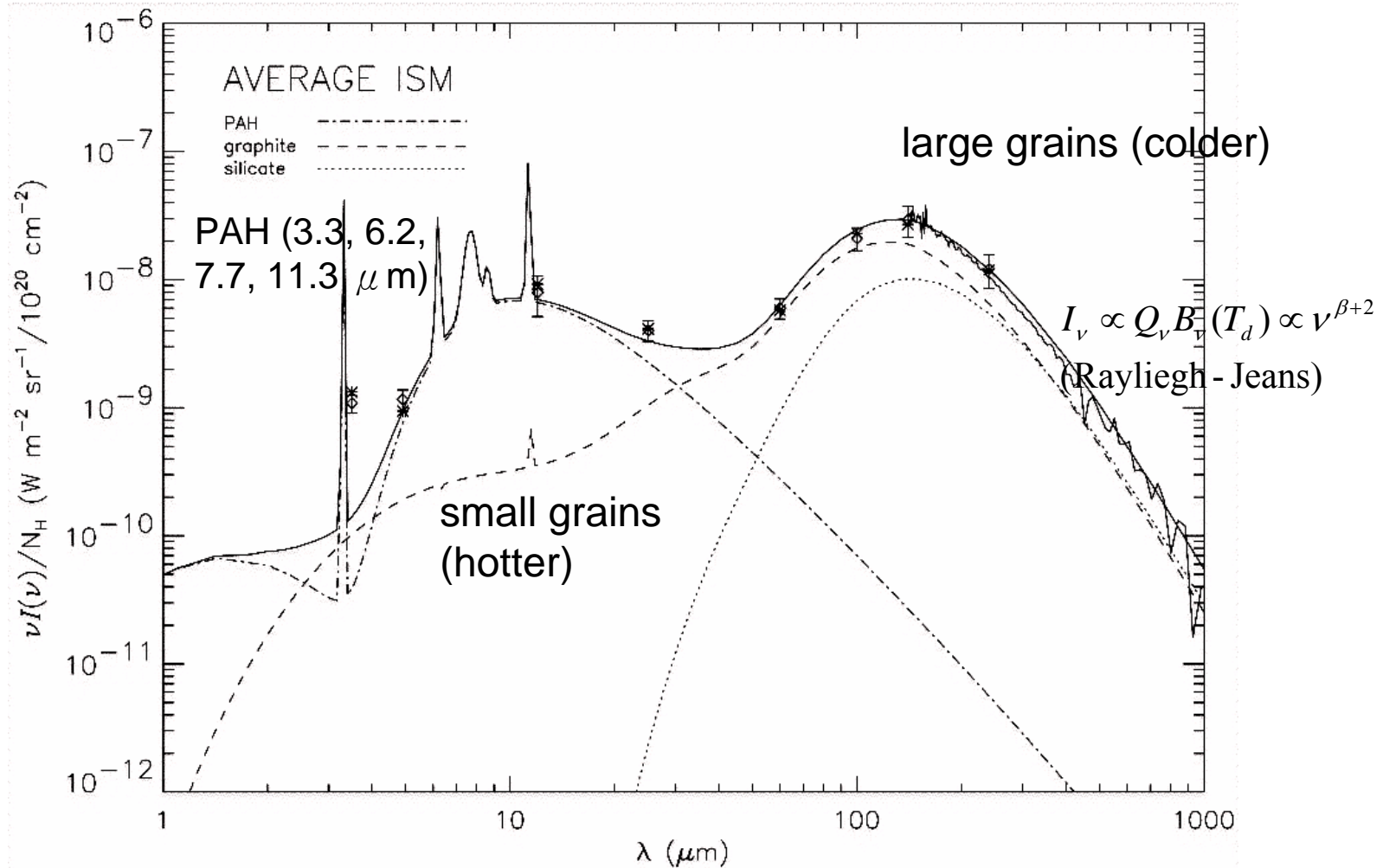
proof : $\frac{dI_\nu}{d\tau_\nu} = S_\nu = B_\nu(T_d) \Rightarrow I_\nu(\tau_\nu) = \tau_\nu B_\nu(T_d)$.

Note that when $x \ll 1$, $Q_{abs} \gg Q_{sca} \Rightarrow \tau_\nu \propto Q_{abs} \propto \nu^\beta$ ($\beta \approx 1-2$)

In the Rayleigh - Jeans regime, $I_\nu \propto \nu^{\beta+2}$

Infrared spectrum of MW

Dwek et al. (1997)



COBE data + Model

measuring the mass content of a protoplanetary disk

we *assume* most of the mass is **cold, molecular gas** (H_2)

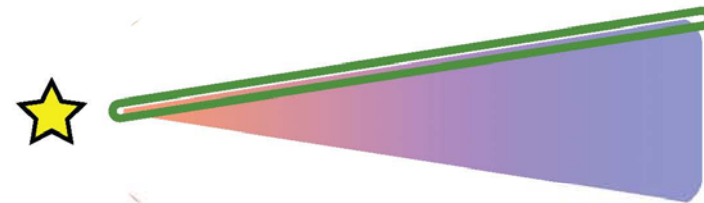


problem: **"dark matter"**

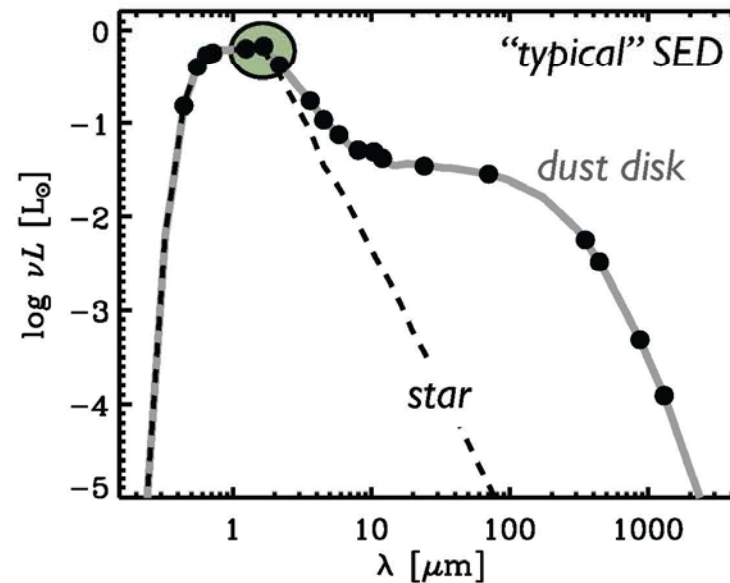
rely on **dust** as a tracer

(it dominates the opacity)

- **scattered light**: flaring/size



[Schneider+ 2003; Kudo+ 2008; Fujiwara+ 2006]



measuring the mass content of a protoplanetary disk

we *assume* most of the mass is cold, molecular gas (H_2)

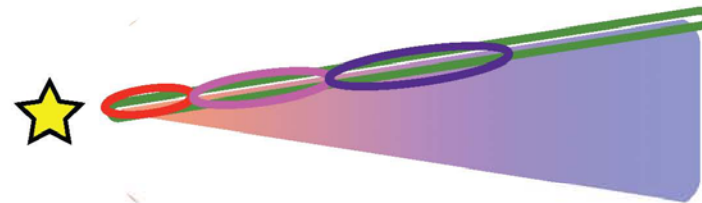


problem: "dark matter"

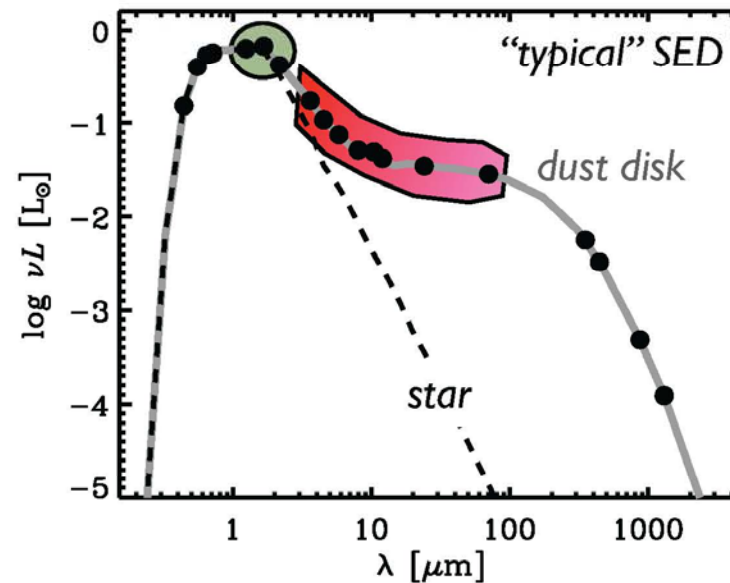
rely on dust as a tracer

(it dominates the opacity)

- scattered light: flaring/size
- IR: flared surface/heating



[Schneider+ 2003; Kudo+ 2008; Fujiwara+ 2006]



measuring the mass content of a protoplanetary disk

we *assume* most of the mass is cold, molecular gas (H₂)



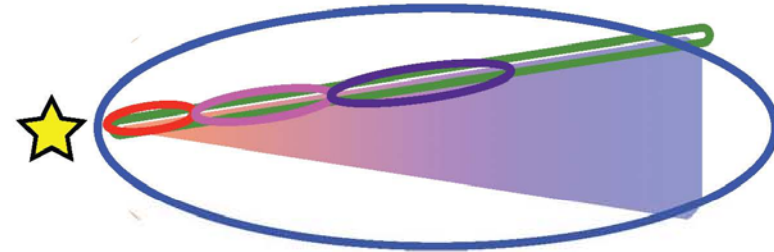
problem: "dark matter"

rely on dust as a tracer

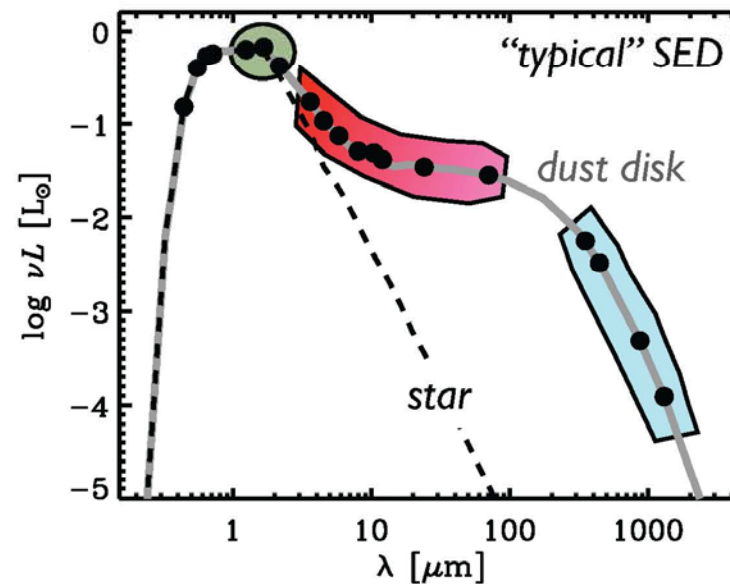
(it dominates the opacity)

- scattered light: flaring/size
- IR: flared surface/heating
- radio: mass in the midplane

$$\text{emission} \propto \kappa_{\nu} \Sigma T$$



[Schneider+ 2003; Kudo+ 2008; Fujiwara+ 2006]

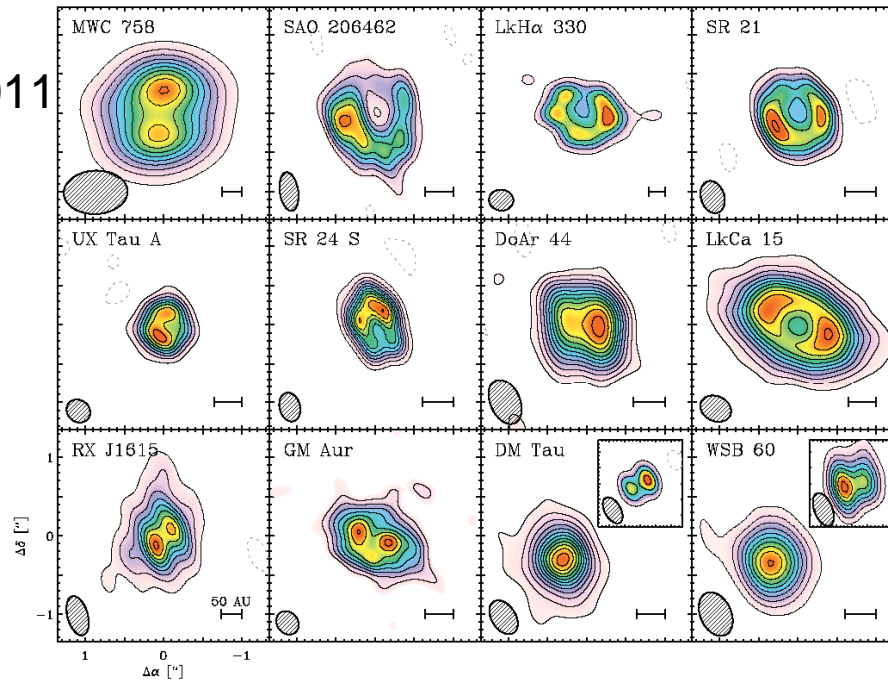


Dust thermal emissions from protoplanetary disks

sub-mm/mm observations:

trace the light (optically thin thermal emissions) directly from large particles (~ sub-mm sized) within a disk

Andrews et al. 2011



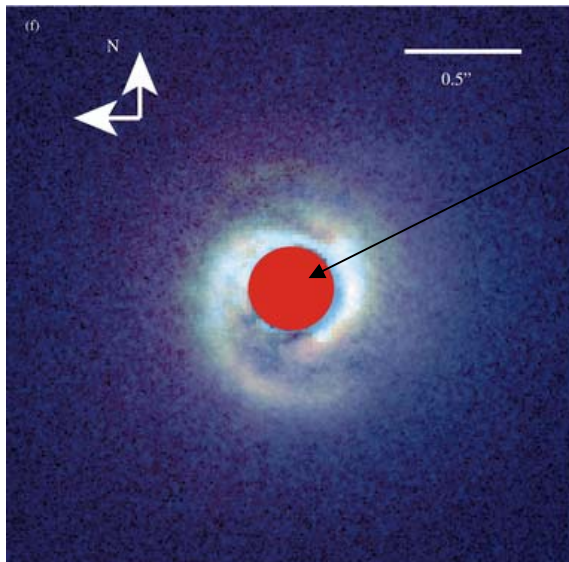
cavity: signposts of a giant planet?

Figure 1. SMA aperture synthesis maps of the $880 \mu\text{m}$ continuum emission from this sample of transition disks. Each panel is $2''7$ on a side (offsets are referenced to the disk centers listed in Table 1; see Section 2) and contains a 50 AU projected scale bar in the lower right for reference. Contours are drawn at 3σ intervals, and the synthesized beam dimensions are marked in the lower left corner (rms noise levels and beam dimensions are provided in Table 2). The inset images for the DM Tau and WSB 60 disks were synthesized with higher angular resolution and are shown to scale.

Polarized scattered light from the surface of a protoplanetary disk

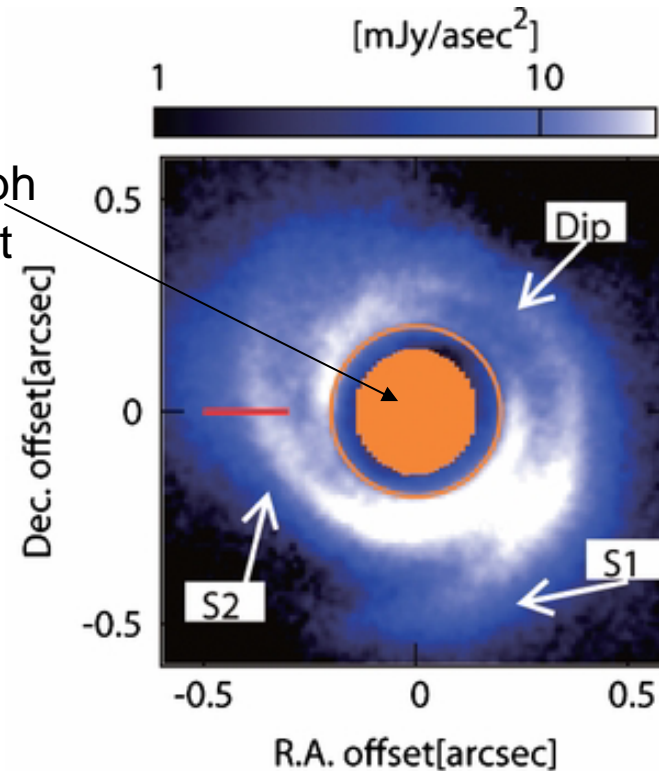
Strategic Explorations of Exoplanets and Disks with Subaru (SEEDS): NIR polarized intensity map ($PI=(Q^2+V^2)^{1/2}$) traces stellar light scattered from small particles ($\sim \mu\text{m}$) on the surface of the disk

“small-scale” spiral structures!
signpost of a planet?



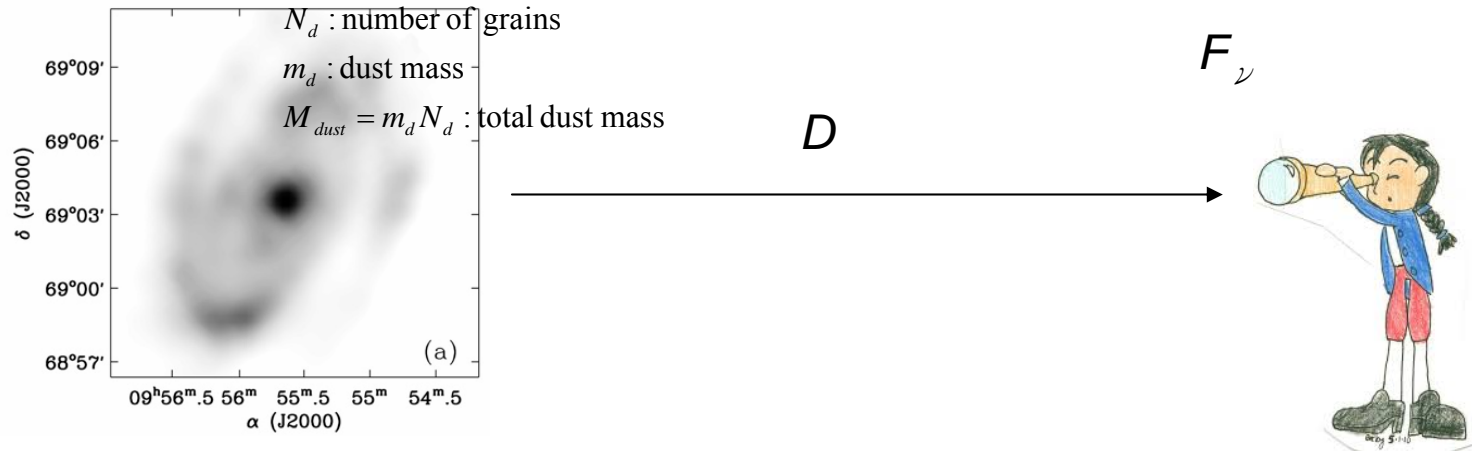
coronagraph to block out light from the central star

Grady et al. 2013: MWC 758
0.1" ~ 20-28 AU



Muto et al. 2012: SAO 206462
0.5" ~ 70 AU

Dust mass estimate



If the object is optically thin at low freq ν (e.g. FIR, sub - mm)

$$4\pi D^2 F_\nu = \dot{E}_{emit,\nu} N_d = 4\pi\sigma_{abs} B_\nu(T_d) N_d = 4\pi m_d \kappa_\nu B_\nu(T_d) N_d$$

$$\Rightarrow M_{dust} = \frac{F_\nu D^2}{\kappa_\nu B_\nu(T_d)}, \quad \text{where } \kappa_\nu = \frac{\sigma_{abs}}{m_d} = \frac{\pi a^2 Q_{abs}(a,\nu)}{(4/3)a^3 s} = \frac{3Q_{abs}(a,\nu)}{4as},$$

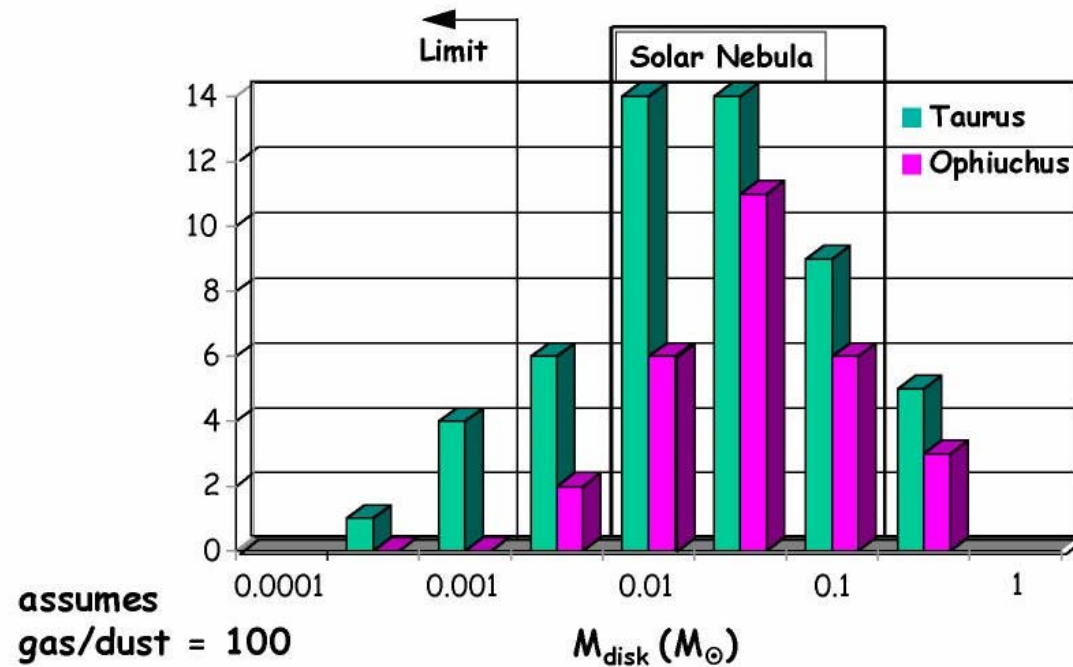
where s is the mass density of a grain.

$Q_{abs}(a,\nu)/a$: independent of a for $a \ll \lambda$.

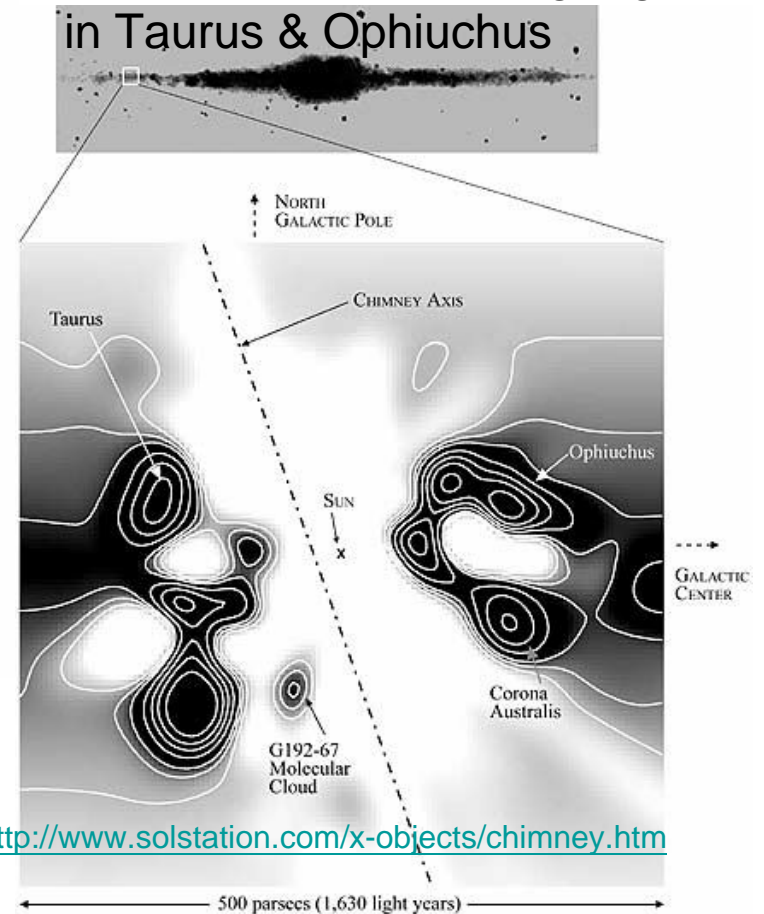
Dust mass is insensitive to the grain size distribution (as long as $a \ll \lambda$).

mass of protoplanetary disks

Beckwith 1999: based on optically thin dust thermal emission at sub-mm



locations of star forming region
in Taurus & Ophiuchus



Linear polarization by Rayleigh scattering

A dipole moment of a molecule/grain with size smaller than λ of incident radiation can be induced. The phenomenon is just analogous to the Thomson scattering.

The intensity component parallel to the scattering plane is reduced by $\cos^2 \theta$, where θ is the scattering angle. Hence, the degree of linear polarization for single scattering is

Let I_{\perp} and I_{\parallel} be the intensity in and normal to the scattering plane, respectively.

$$\pi = \frac{I_{\perp} - I_{\parallel}}{I_{\perp} + I_{\parallel}} = \frac{1 - \cos^2 \theta}{1 + \cos^2 \theta}.$$

Multiple scattering washes out the polarization signal.

Since $Q_{sca}(a, \nu)$, π is the wavelength - dependence: generally, π rises from short λ , reaches a maximum value at λ_{\max} and then fall to longer λ .

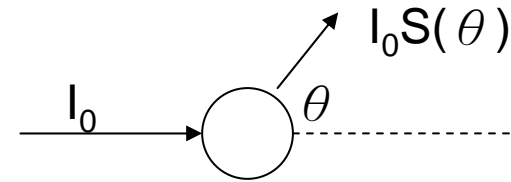
Astronomical applications: reflection nebulae, protoplanetary disk surface,
planet/brown dwarf atmosphere.

Forward scattering

For sufficiently small grains ($a \ll \lambda$), the Rayleigh scattering (cf. the Thomson scattering) gives the angular distribution of the radiation

$$S(\theta) = \frac{1 + \cos^2 \theta}{2}$$

where θ is the angle from the propagation direction of the incident beam. This gives us a characteristic "dog bone" scattering pattern. Small grains are (to within a factor of 2) isotropic scatterers. The factor of 2 is the dog bone pattern. Note that the missing half at right angles to the propagation direction is the portion of incident light which had no polarization component which aligns with the characteristic polarization which must exist for light detected at a right angle from a scattering body.



We consider the model in which an infinite plane wave passes through an aperture, is focused by an infinite lens, and shines on a wall. In this model, as the slit aperture widens (a increases), then the diffraction pattern narrows. Thus, for larger grain sizes, there is more forward scattering than in other directions. The fitting formula for the power pattern for large grains is (Heyney - Greenstein scattering function)

$$S(\theta) = \frac{1 - g^2}{1 + g^2 - 2g \cos \theta}, \quad \text{where } g \equiv \langle \cos \theta \rangle = \frac{\int S(\theta) \cos \theta d\Omega}{\int S(\theta) d\Omega}.$$

$g = 1, 0, -1$ means forward, isotropic, and backward scattering, respectively.

Forward scattering can actually increase the intensity of light in some areas if there were no scattering at all. If particles are smaller than the wavelength of light, there is isotropic scattering.

For larger particles, the power is more concentrated in the perfectly forward and backward directions.

This is why, where there is fog, you dim your headlights. The larger scattering particles in the fog actually increases the intensity of light reflected back at you and at oncoming cars.

Forward scattering

A. Evans: The Dusty Universe

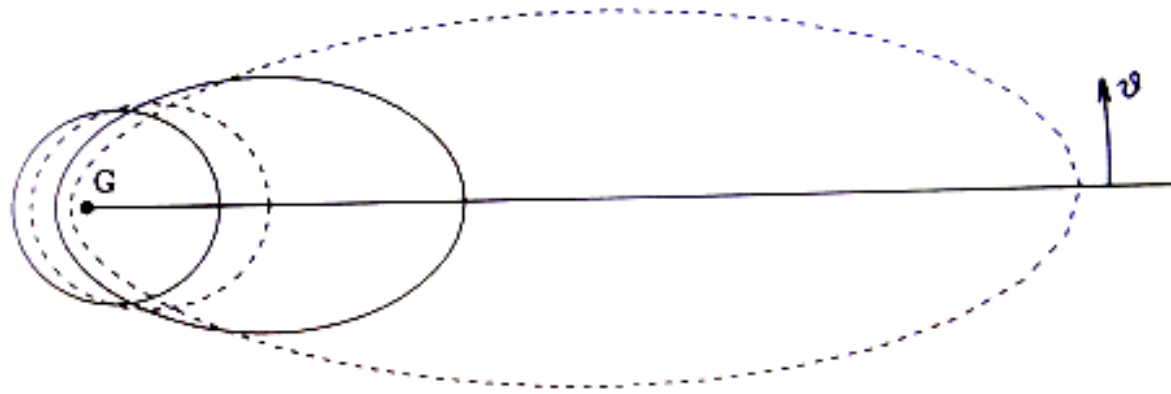
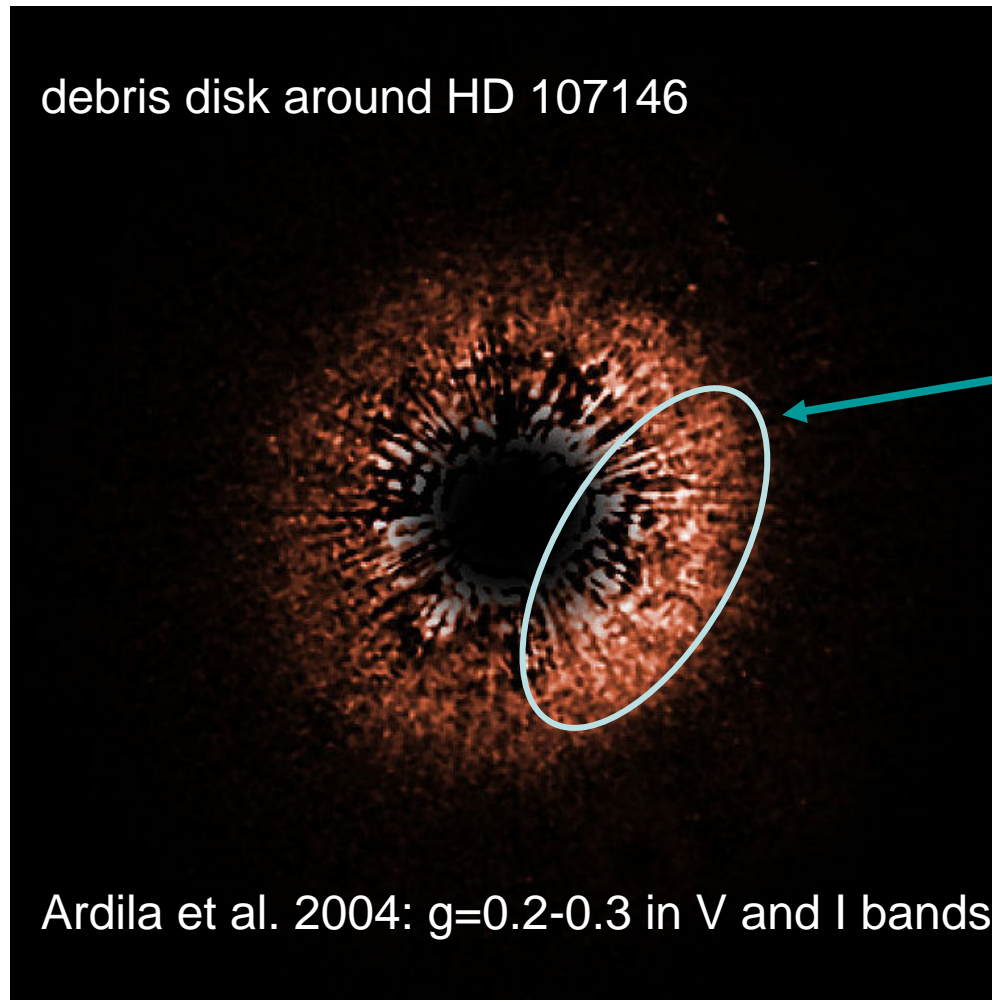


Figure 3.8: The Heyney-Greenstein scattering function for scattering by a grain at G; radiation is incident from the left. The polar diagrams are (in order of increasing ellipticity) for $g = 0.1, 0.2, 0.4, 0.6$.

Example of forward scattering



forward scattering, suggesting this part of the debris disk tilts toward us

Linear polarization by extinction

Extinction by spherical grains does not preferentially absorb or scatter radiation having any specific state of polarization; non-spherical grains (or non-isotropic electric properties) will however do so.

$I_{\parallel} = I_{\parallel}^{(0)} \exp(-\tau_{\parallel})$, where \parallel denotes E field parallel to the grain axis

$I_{\perp} = I_{\perp}^{(0)} \exp(-\tau_{\perp})$, where \perp denotes E field normal to the grain axis

Assume $I_{\parallel}^{(0)} = I_{\perp}^{(0)}$ for incident unpolarized light and if τ_{\parallel} and $\tau_{\perp} \ll 1$,

$$\pi = \frac{I_{\parallel} - I_{\perp}}{I_{\parallel} + I_{\perp}} = \frac{I_{\parallel}^{(0)} \exp(-\tau_{\parallel}) - I_{\perp}^{(0)} \exp(-\tau_{\perp})}{I_{\parallel}^{(0)} \exp(-\tau_{\parallel}) + I_{\perp}^{(0)} \exp(-\tau_{\perp})} \approx \frac{\tau_{\perp} - \tau_{\parallel}}{\tau_{\perp} + \tau_{\parallel}} = \frac{Q_{ext,\perp} - Q_{ext,\parallel}}{Q_{ext,\perp} + Q_{ext,\parallel}}$$

For normal incidence & infinitely long cylindrical grains,

$$Q_{ext,\parallel} \approx -\frac{\pi x}{2} \text{Im}(n^2 - 1), \quad Q_{ext,\perp} \approx -\pi x \text{Im}\left(\frac{n^2 - 1}{n^2 + 1}\right)$$

Extinguished starlight is linearly polarized, and the degree of polarization is well correlated with the visual extinction.

Dust alignment & magnetic fields

Off - center collisions of grains with atoms and molecules will impart rotational as well as translational kinetic energy. Random spin of a grain due to elastic collisions with gas : $(1/2)I\langle\omega_{th}^2\rangle \sim kT_{gas}$

Consider a cylindrical grain of mass $m_d \sim 6 \times 10^{-21}$ g and length $l \sim 0.1 \mu\text{m}$.

The moment of inertia $I \approx m_d l^2 / 3$. If $T_{gas} \approx 100\text{K}$, $\omega_{th} \approx 3 \times 10^5$ 1/s. But how long to reach the large ω_{th} ?

The spinning up timescale $\tau_{spin} \sim$ time over which the grain collides with its own mass of gas

$$m_H (n_H a l v_g) \tau_{spin} \sim m_d = \pi a^2 l \rho \Rightarrow \tau_{spin} \sim \frac{\pi a \rho}{m_H n_H v_g} \sim 10^7 \left(\frac{\rho}{2 \text{ g/cm}^3} \right) \left(\frac{T_{gas}}{100 \text{ K}} \right)^{-1/2} \text{ years.}$$

In addition, radiative torques due to ISRF can also induce spin - up (Draine & Weingartner 1996, 1997)

Dust alignment is not well understood. Here we introduce the Davis - Greenstein mechanism (1957, ApJ, 114, 206). The model is based on the paramagnetic dissipation that is experienced by a rotating grain.

Magnetic properties of a grain under an external B - field ($B = B_0 \exp(i\omega t)$) if $T_d < T_{Curie}$:

$$B = \mu H = (1 + 4\pi\chi_m)H = H + 4\pi M$$

$$M = \chi_m H = (\chi_{m,R} + i\chi_{m,I})H$$

In general, $\chi_{m,I} \propto \omega / \omega_0$, where ω_0 depends on the grain magnetic properties.

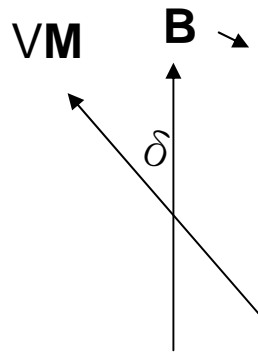
If $\chi_{m,I} \ll 1$ (i.e. grains are spinning slowly or not spinning), the grain behaves as though it were in a static B - field. The magnetic dipole moment in which the para - magnetism of the grain originate can "keep up with" the changing B - field. Nothing significant will happen to the grain random spins.

Dust alignment & magnetic fields

If $\chi_{m,I} \gg 1$ (i.e. a grain spinning fast), the dipole fails to keep up with the external \mathbf{B} -field and therefore they lag behind the rotation. Consequently, \mathbf{M} and \mathbf{B} are not parallel. Let V be the volume of the grain and thus $V\mathbf{M}$ is the magnetic dipole moment. There is a retarding torque $V(\mathbf{M} \times \mathbf{B})$, whose magnitude $\approx kV |\mathbf{B}|^2 \omega$, where k absorbs all the constants in the magnetic moment, which acts to damp out any rotation about any axis that has a component normal to the \mathbf{B} -field. Simply speaking, a grain prefers to spin with its spin axis parallel to \mathbf{B} : in this orientation, \mathbf{M} is constant in the grain. For orthogonal spin, \mathbf{M} fluctuates and thus dissipates rotational KE. This occurs on a timescale

$$\tau_{align} \approx \left| \frac{\omega}{\dot{\omega}} \right| = \frac{I}{kVB^2}$$

Consider spin axis of the grain is out of page.
In the co-rotating frame of the grain:



$$\delta = \arctan\left(\frac{\chi_{m,I}}{\chi_{m,R}}\right):$$

lag angle due to $\chi_{m,I}$

Linear Polarization: reddening starlight & sub-mm dust emissions

Grains absorb and emit the electric field of radiation preferentially along their long axes. As long as the gas density is low enough to avoid spin randomization by collisions with gas.

- polarization by extinction gives polarization parallel to **B**
- polarization from dust thermal emission should lie on a plane normal to **B**

Galactic magnetic fields

Polarization vectors are only seen as projected in the plane of the sky.
Large-scale ordered field (as seen from its plane-of-the-sky
Projection) along the Galactic plane.

Fosalba
et al.2002

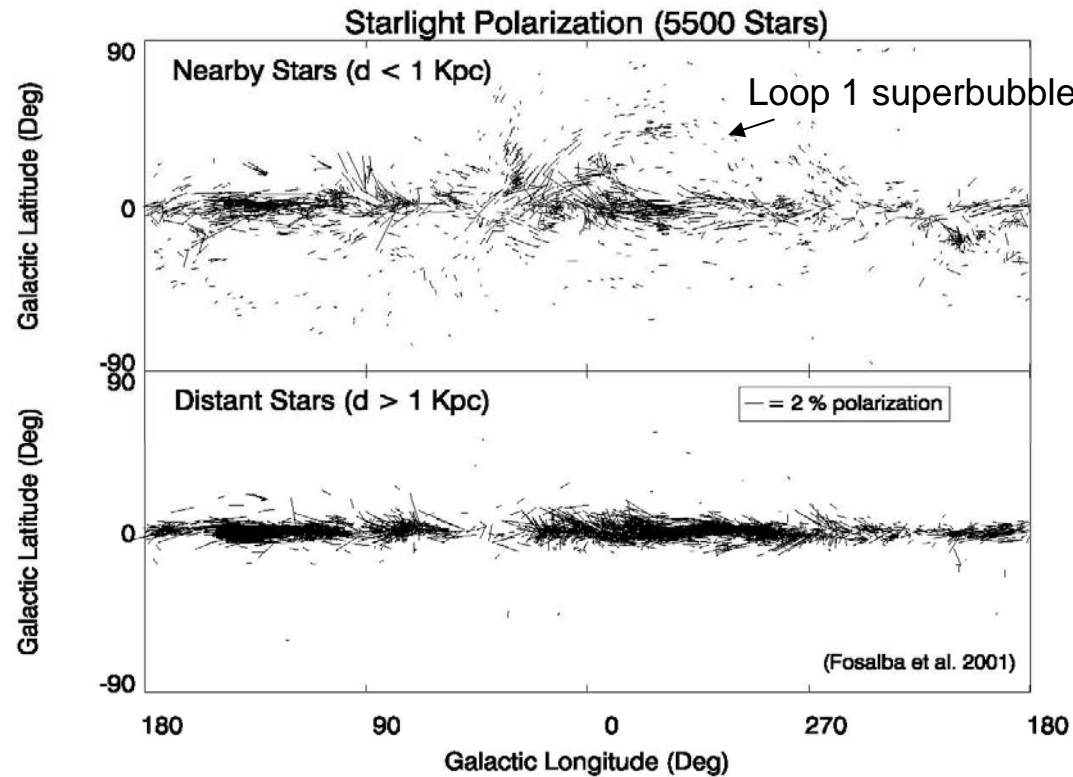
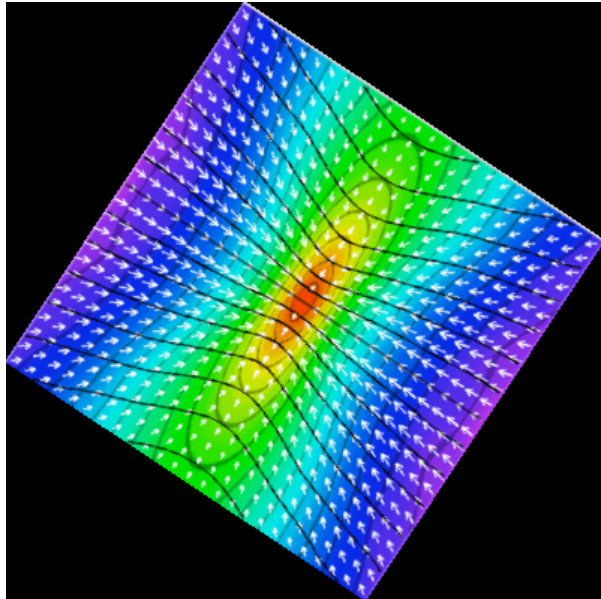


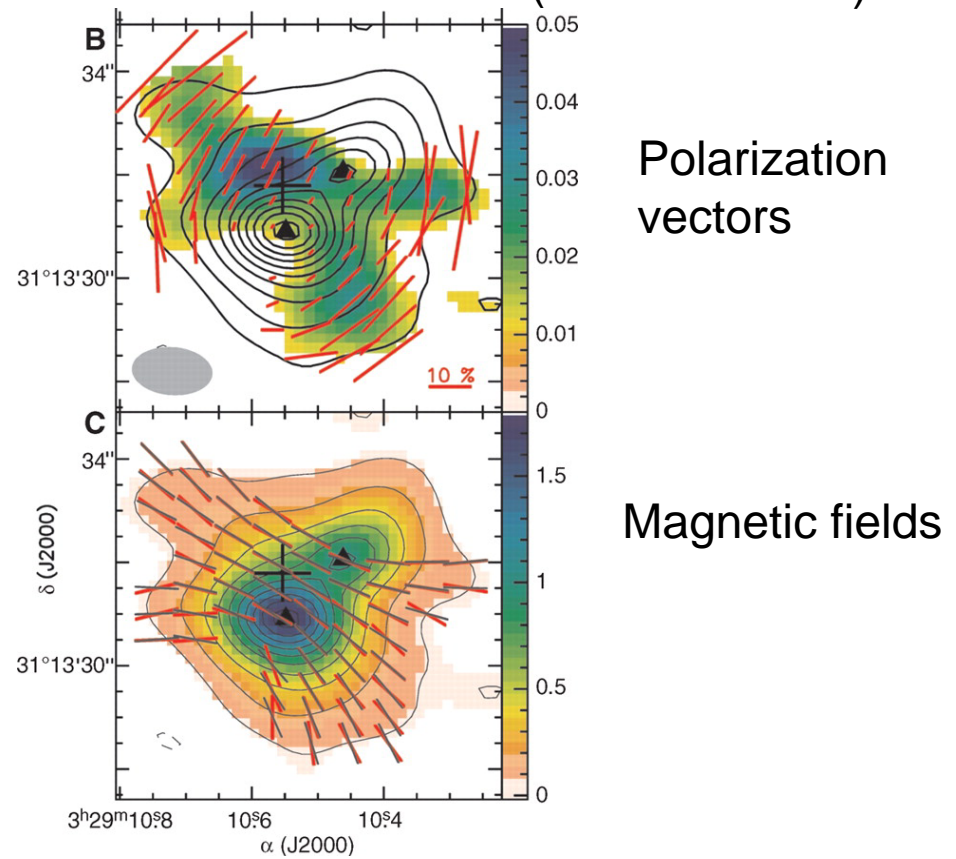
FIGURE 2. Starlight polarization vectors in Galactic coordinates for a sample of 5513 stars. The upper panel shows polarization vectors in local clouds, while the lower panel displays polarization averaged over many clouds in the Galactic plane. The length of the vectors is proportional to the polarization degree and the scale used is shown in the lower panel.

Magnetic fields in a protostellar system

scenario



Girart, Rao, Marrone 2006:
NGC 1333 IRAS4: low-mass protostellar system
Polarized dust emission (SMA 345 GHz)



Radiation forces on dust

We have learned that dust can absorb, scatter, and reemit radiation, but these processes should result in forces on the dust. Ref: Burns et al. 1979; Gustafson 1994

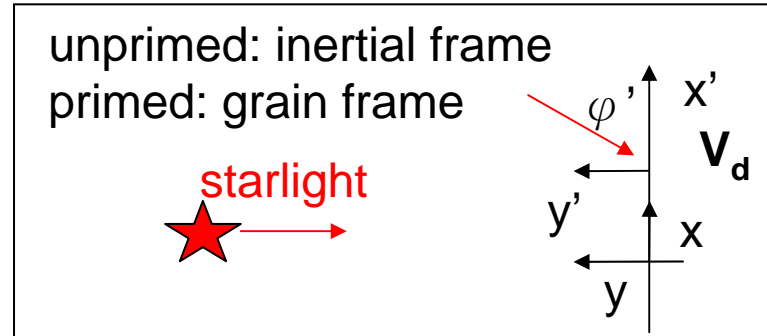
$F_{\text{rad}} = \text{radiation pressure } (\mathbf{r}) + \text{Poynting-Robertson drag } (\theta)$

Poynting-Robertson drag

A dust grain orbiting a star experiences an orbital decay due to aberration of starlight as seen from the grain :

$$\text{Lorentz transformation of velocity} \Rightarrow v_x = \frac{v'_x + V_d}{1 + v'_x \frac{V_d}{c^2}}$$

$$\Rightarrow \frac{v_x}{c} = \frac{v'_x/c + V_d/c}{1 + v'_x \frac{V_d}{c^2}} \Rightarrow \cos \phi = \frac{\cos \phi' + \beta}{1 + \beta \cos \phi'}, \quad \text{where } \beta = \frac{V_d}{c} \text{ and } \phi \text{ and } \phi' \text{ are the angles between the}$$



incident starlight and the orbital motion of the grain in the inertial & grain frames, respectively.

Because $\phi = \pi/2$, $\cos \theta = 0 \Rightarrow \cos \phi' = -\beta$, as expected for the case in the non-relativistic regime.

Given the cross section σ , the stellar luminosity L_* , the distance r , the grain angular momentum J ,

$$\frac{dJ}{dt} = r \frac{L_*}{4\pi r^2 c} \sigma \cos \phi' = -\frac{L_* \sigma (m_d r V_d)}{4\pi r^2 m_d c^2} = -\frac{L_* (\pi a^2 Q)}{4\pi r^4 m_d c^2} J$$

$$\Rightarrow \tau_{PR} = \frac{J}{\dot{J}} \approx 10^6 \text{ yr} \left(\frac{r}{50 \text{ AU}} \right)^2 \left(\frac{a}{\mu\text{m}} \right) \left(\frac{\rho}{\text{g/cm}^3} \right) \left(\frac{1}{Q} \right) \left(\frac{L_*}{L_{sun}} \right)^{-1},$$

where Q can be shown to equal $Q_{abs} + Q_{sca} (1 - g)$

NB: If the initial orbit is not circular, P-R drag will also circularize the orbit.

radiation pressure

$$F_{rad} = (\pi a^2 Q) \frac{L_*}{4\pi r^2} \frac{1}{c}$$

$$\beta \equiv \frac{F_{rad}}{F_{grav}} = \frac{F_{rad}}{GM_* m_d / r^2} \approx 0.575 \frac{\text{g/cm}^3}{\rho} \frac{\mu\text{m}}{a} \frac{L_*}{L_{sun}} \frac{M_{sun}}{M_*}$$

i.e. a grain sees a "less massive" star with the mass reduced by a factor $(1 - \beta)$.

In general, the grain is not orbiting on a circular orbit. In the non-relativistic limit $|\mathbf{v}_d| \ll c$ (Burns et al. 1979):

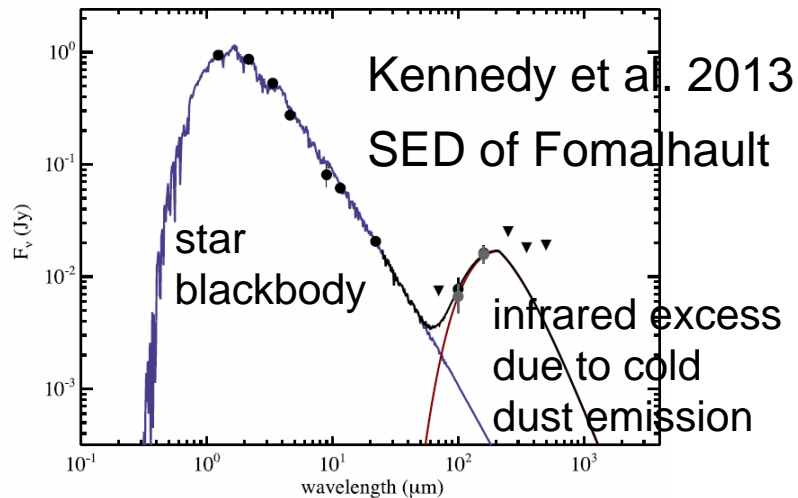
$$\mathbf{F}_{rad} = (\pi a^2 Q) \frac{L_*}{4\pi r^2} \frac{1}{c} \left[\left(\underset{\substack{\uparrow \\ \text{radiation} \\ \text{pressure}}}{1 - \frac{\dot{r}_d}{c}} \right) \hat{r} - r \underset{\substack{\uparrow \\ \text{Poynting-robertson} \\ \text{drag}}}{\dot{\theta}_d} \hat{\theta} \right]$$

debris disk around

Fomalhaut

(北落師門)

$$F_{rad} \propto \beta \propto \frac{1}{a}$$



debris disk is postulated as the 2nd generation of dust from the collisions between planetesimals which are leftover from the proto-planetary disk. Similar to the debris from asteroid and Keiper belt objects in the Solar System.

